Food Chemistry: X 23 (2024) 101622

Contents lists available at ScienceDirect

Food Chemistry: X

journal homepage: www.sciencedirect.com/journal/food-chemistry-x

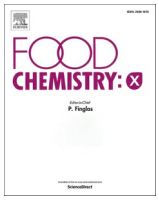

Effect of electrohydrodynamic (EHD) drying on active ingredients, textural properties and moisture distribution of yam (*Dioscorea opposita*)

Jie Zhang [a], Changjiang Ding [a,b,*], Jingli Lu [a,**], Jie Zhu [b], Wurile Bai [a], Peng Guan [a], Zhiqing Song [b], Hao Chen [a]

[a] College of Science, Inner Mongolia University of Technology, Hohhot 010051, China
[b] College of Electric Power, Inner Mongolia University of Technology, Hohhot 010051, China

ARTICLE INFO

Keywords:
Electrohydrodynamic (EHD) drying
Yam
Active ingredients
Textural property
Low-field nuclear magnetic resonance (LF-NMR)

ABSTRACT

This paper systematically investigates the changes in material properties during electrohydrodynamic (EHD) drying, the discharge characteristics of the EHD system as well as the active ingredients, textural properties (hardness, adhesiveness, etc.) and moisture distribution of yam under EHD, air drying and hot air drying were investigated. The results showed that the active particles and the ionized wind generated during the discharge process of the electrohydrodynamic drying device had a significant effect on the drying. Compared to thermal drying, 21 kV drying resulted in the most complete cellular structure, the best internal bound water content as well as textural properties of yam. It played a positive role in the retention of internal nutrients in yam, and the total phenol and allantoin contents were increased by 25.74% and 81.99%, respectively. These results elucidate the advantages of electrohydrodynamic drying in yam drying and provide a reference for the application of EHD in drying.

1. Introduction

The yam is one of the traditional medicinal and edible foods in China. The edible part is its rhizome, which contains a variety of nutrients, including protein, total phenol, allantoin and so on, and has high edible value and medicinal value. Studies showed that eating yam helps to enhance digestion and absorption, improve immunity and prevent cardiovascular diseases (Zhang, Ding, et al., 2023; Zhang, Zheng, et al., 2023). However, yam is a seasonal food, with a moisture content of over 70%, which is easy to rot and deteriorate after long-term storage. Therefore, drying treatment is very important.

Drying mainly reduces water activity by reducing the water content of materials, prolongs the shelf life of materials, maintains the stability of nutrients, and avoids microbial contamination during storage (Xiao et al., 2015). At present, the common drying methods of yam include natural drying (Ju et al., 2015), hot air drying (Ju et al., 2016), vacuum freeze-drying (Chen, Lu, et al., 2017; Chen, Tian, et al., 2017), and microwave drying (Chen, Lu, et al., 2017; Chen, Tian, et al., 2017). Natural drying has a low cost but a long drying time, and the drying process is easily affected by weather conditions. Hot air drying is fast, but too high a temperature will cause the color change of materials and the loss of nutrients. The speed of drying is high in vacuum freeze-drying and microwave drying, but the equipment must be expensive and energy consumption necessary. The drying methods are not entirely suitable for the requirements of drying by-products. To promote the development of the drying industry, it is very important to explore new drying technology.

Electrohydrodynamic (EHD) drying technology is a kind of non-thermal drying technology that utilizes the joint action of a non-uniform electric field and ion wind for drying. Among them, a non-uniform electric field produces high-energy ions into the material inside, and material molecules and water molecules interact with energy transfer and charge exchange, resulting in an increase in the energy of the water molecules, chain molecular group of water molecules between the hydrogen bond is broken to promote the migration of water molecules from the inside of the material to the surface of the material (Ni, Bi, et al., 2023; Ni, Wang, et al., 2023; Wang et al., 2023). Ionic wind acts on the material surface, accelerating the evaporation of water molecules on the material surface. EHD drying, which is low-temperature drying, is one of the perfect alternatives to hot air drying (HAD). This is because it

* Corresponding author at: College of Science, Inner Mongolia University of Technology, Hohhot 010051, China.
** Corresponding author.
E-mail addresses: ding9713@163.com (C. Ding), lujingli2004@163.com (J. Lu).

https://doi.org/10.1016/j.fochx.2024.101622
Received 26 April 2024; Received in revised form 19 June 2024; Accepted 2 July 2024
Available online 4 July 2024

provides higher nutrient content and a more attractive color. Apple slices and grape pomace dried by EHD have been reported to have significant advantages in terms of color, shrinkage and retention of phenolics compared to hot air drying (Paul & Martynenko, 2022; Martynenko & Kudra, 2016a, 2016b; Martynenko & Zheng, 2016). After EHD drying, the apricot microstructure was better preserved and the color was more vibrant (Polat & Izli, 2020). Ozone produced by EHD drying inhibits the onset of lipid oxidation and effectively promotes the volatilization of key volatile aldehydes from bee pollen (Ni et al., 2023). However, the effect of water loss during EHD drying on texture is unknown.

Since the texture of dried products accurately reflects their mechanical and microstructural properties, it is one of the most important quality attributes for consumers to evaluate dried food products (Martynenko & Janaszek, 2014). Different drying methods have different effects on the microstructure of dried products. Irreversible shrinkage and deformation of materials caused by water loss will lead to changes in various texture parameters. Sensory analysis is often used to characterize the texture of dried foods, but it is highly subjective. Therefore, in recent years, texture meters have been commonly used in the field of food analysis instead of sensory analysis. Texture analysis is mainly used to measure the mechanical properties of food related to human sensation, including hardness, chewiness, adhesiveness and other indicators. Compared with sensory analysis, texture analyses offer advantages such as objectivity and stability, as well as convenience. Krokida et al. (2000) found that the moisture content during drying had a significant effect on the mechanical and structural properties of apple slices, as dehydration resulted in softening of the cell walls of the slices, and the springiness of the slices was reduced as the moisture content decreased. Similarly, Ferreira et al. (2007) found that solar drying of pears resulted in cell shrinkage and disruption of cell wall integrity, the adhesiveness of pears was lost and hardness and fracturability were significantly reduced. Drying affects the microstructure and texture of fruits and vegetable tissues because it is a complex process. Many complex biochemical reactions occur during water removal.

Low-field nuclear magnetic resonance (LF-NMR) explains the distribution state and migration of water in a sample from a microscopic point of view by analyzing the transverse relaxation time (T_2) changes of hydrogen nuclei in different states of existence in a magnetic field (Chen et al., 2017). This technique is generally not affected by the size and shape of the sample and has the advantages of high efficiency, rapidity, high precision and non-invasion (Guan et al., 2023). In recent years, it has been widely used in the field of food science to detect the moisture distribution of fruits and vegetables during ripening, processing and storage. Chen et al., (2023) used a low-field NMR technique and found that hot air drying and infrared drying forced the free water in peanuts to be removed first, and then some of the free water was converted to loosely bound water. Mowafy et al. (2024) found that blanching resulted in the hydrolysis of the potato cell wall, which resulted in the release of some of the bound water into the intracellular space, and the T_{21} peak area was reduced. Lv et al., (2017) tested the moisture status in six vegetables using the LF-NMR method and found a direct correspondence between NMR signal amplitude and moisture content, which can be used to predict the drying endpoint. Until now no research has been done on the application of the LF-NMR technique to study EHD drying of yam.

Most scholars have focused on the optimization of EHD equipment and its effect on the drying characteristics of by-products. No study has been found on the effect of EHD on the drying quality, mechanical properties and internal moisture distribution of yam. Therefore, the objectives of this study were to systematically investigate: (1) the effects of different drying methods (EHD, AD, and HAD) on the drying rate of yam; (2) the effects of EHD, AD, as well as HAD on the quality parameters of yam (e.g., total phenol content, allantoin content); and (3) to elucidate the variations in textural properties and moisture distribution of yam under different drying methods.

2. Materials and methods

2.1. Experimental materials and methods

The variety of yam used for the experiments was iron stick yam. Fresh yam was purchased and stored in a refrigerator at −4 °C for further experiments. The initial moisture content of yam was measured as (77.61 ± 0.88) % by a moisture rapid detector (SH10A, Shanghai, China). The outer skin of fresh yam was removed and cut into cylindrical slices of 12 mm diameter and 3 mm thickness. The mass of the yam slices was measured every 0.5 h using an electronic balance (BS124S, Shanghai, China). The drying was finished when the moisture content of the dry base of yam was 10% by default. The specific experimental method is shown in Scheme 1.

2.2. Drying process

HAD was performed by placing Petri dishes containing yam slices individually in a hot air drying oven (Shanghai, China) at a constant temperature of 60 °C. The drying temperature of the AD and EHD was 20 ± 2 °C, relative humidity 39 ± 1%, and natural air velocity 0 m/s. The EHD drying equipment consists of a high-voltage power supply, a needle-plate electrode and an AC voltage controller. The AC voltages were set to 13 kV, 17 kV, and 21 kV, respectively. The top electrode was a multiple sharp pointed needles electrode that was connected to a power source, and the spacing between two adjacent needles was 40 mm. The lower electrode was a metallic plate on which the yam samples to be dried were placed with an area of 1000 mm × 450 mm. The distance from the multiple needles to the metallic plate electrode was 80 mm.

2.3. Measurement of electric field discharge characteristics

The discharge process of EHD at different voltages (13 kV, 17 kV & 21 kV) was processed using ICCD (DH334T-18 U-E3, UK). Plasma emission spectra in the band range of 200–900 cm^{-1} were obtained. The discharge morphology under different voltages was photographed by a camera in a dark environment. The voltage and current waveforms at different voltages at a discharge frequency of 50 Hz were detected using an oscilloscope (RIGOL MSO5204, China), a high-voltage probe (Tektronix P6015A, USA), and a current monitor (Pearson, USA). Ion wind speed was measured using a thermal anemometer probe (Testo 405i, Germany) at different voltages, and the results were averaged over 60 measurements. The discharge power of the main body of the EHD discharge device at different voltages was derived according to the Lissajous method. A sampling capacitor C_M is connected in series with the ground terminal of the discharge device, then the charge Q transmitted by the measured capacitor is:

$$Q = C_M \times U_M \tag{1}$$

where U_M is the voltage across the capacitor and the current I flowing through the capacitor C_M is:

$$I = \frac{dQ}{dt} = \frac{d(C_M U_M)}{dt} = C_M \bullet \frac{dU_M}{dt} \tag{2}$$

The discharge voltage U_T is:

$$U_T = U_H - U_M \approx U_H \tag{3}$$

where U_H is the voltage of the whole circuit. Because of $U_H \gg U_M$, so the instantaneous power P is:

$$P = U_T \times I_T \approx U_H \times C_M \bullet \frac{dU_M}{dt} \tag{4}$$

The average power P of the EHD discharge unit is:

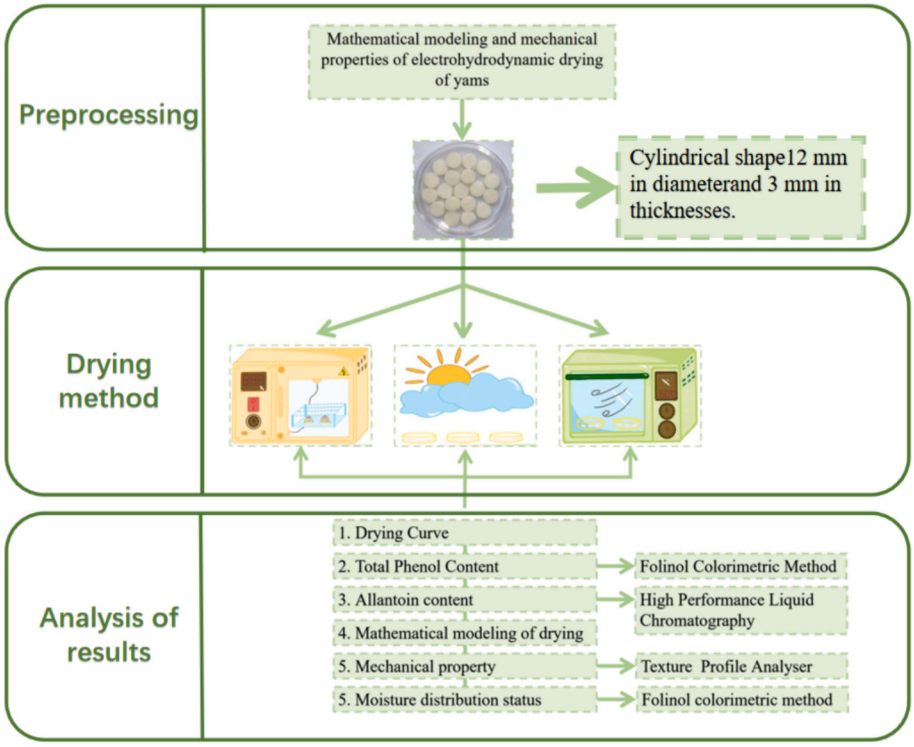

Scheme 1. Schematic diagram of the experimental procedure and drying model.

$$P = \frac{1}{T}\int_0^T U_T I_T dt = f \times C_M \times \int_0^T U_H dU_M = f \times C_M \times S \quad (5)$$

where f is the frequency of the AC power supply, S is the area of the Lissajous graph, and C_M is the sampling capacitance. The discharge power of the EHD discharge device is proportional to the size of the area of the Lissajous graph.

2.4. Drying curve

The dry basis moisture content and water content ratio of yam tablets during drying were calculated by the formula (Ni et al., 2020):

$$M_i = \frac{m_i - m_g}{m_g} \times 100\% \quad (6)$$

$$MR = \frac{M_i - M_e}{M_0 - M_e} \quad (7)$$

where M_i is the dry basis moisture content of yam tablets dried to t_i time (unit: g water/g solid), m_i is the mass of yam tablets dried to t_i time (unit: g), m_g is the dry mass of yam tablets (unit: g), MR is the moisture content ratio of yam tablets, M_e is the equilibrium moisture content of yam tablets, and M_0 is the moisture content of yam tablets at t_0 time. Usually, the value of M_i is negligible compared to M_0 (Chauhan et al., 2021). Therefore, the moisture content ratio equation is given as:

$$MR = \frac{M_i}{M_0} \quad (8)$$

2.5. Determination of total polyphenol content (TPC)

The total phenol content of yam under different drying methods was determined using the forintol colorimetric method. The method was based on Ferreira et al., (2004) for the preparation of Folin-Ciocalteus (FC) colorant.

The yam samples dried by different drying methods were crushed and screened by a 60 mesh sieve for later use. Then weighed the 0.20 g sample and added 50 mL distilled water. Kept the temperature in a boiling water bath at 100 °C for 30 min, took it out, let it cool, then fixed the volume, and filtered the filtrate for later use. Took 2.5 mL of the extract in a 50 mL centrifuge tube and added 30 mL of 60% ethanol solution. After ultrasonic treatment for 10 min, the volume was adjusted to 40 mL with 60% ethanol solution. Sucked 1.0 mL of filtrate (if the total phenol content is too high, it can be diluted appropriately) or a standard solution of gallic acid monohydrate, and added 2.5 mL of FC chromogenic agent (added 1 time distilled water to dilute) with graduated pipette respectively. 15% sodium carbonate solution 2.5 mL, constant volume to 10 mL with distilled water, mixed well, water bath at 40 °C for 60 min, let stand and cool for 20 min. Determined the absorbance at 778 nm, and calculated the total phenol content of the sample according to the dilution multiple and the concentration found from the standard curve. Therefore, the calculation formula for total phenols in yam is:

$$TPC = CN\frac{0.001V_t}{mV_s} \quad (9)$$

where C is the content of total phenols found from the standard curve, (unit: μg/g); N is the dilution factor, V_t is the total volume of extract (unit: mL); V_s is the amount of liquid taken for the determination (unit: mL); m is the mass of yam tablets; and the unit of total phenol content is mg/g.

2.6. Determination of allantoin content

High-performance liquid chromatography (HPLC) was used to determine the allantoin content in yam samples under different drying methods. After the yam samples were crushed by different drying methods, 10 mL of methanol was added to each 1 g sample. The sample was ultrasonicated for 30 min and then centrifuged, and the supernatant was extracted into a vial for analysis. The specific parameters were modified according to Zhang et al., (2023). The matrix effect was removed by calibration of the matrix standard solution (Song et al.,

2017). After pretreatment, the blank sample is added with a certain amount of standard substance to be tested to correct the test results. Confirm the separation method, and if there is no problem with the peak of the standard product, extract the sample in the same way.

LC conditions: analytical column 50*2.1 mm; mobile phase: 0.1% formic acid, acetonitrile; needle wash solution: 50% methanol in water; flow rate: 0.5 mL/min; column temperature: 25 °C; injection volume: 5 μL; injector temperature: 5 °C; analysis time: 1 min.

MS conditions: Negative Ion Mode; Gas Temp: 350 °C; Gas Flow: 7 L/min; Nebulizer: 30 psi; Capillary: 3500 V; Sheath Gas Heater: 300 °C; Sheath Gas Flow: 8 L/min; Delta EMV: 200.

2.7. Textural properties

A texture analyzer was used to determine the textural properties of yam samples under different drying methods. The texture analyzer was used to obtain characteristic curves by simulating the chewing motion of the human mouth and performing two compression tests on the dried yam products. Relevant parameters of textural properties, such as hardness, resilience, springiness, adhesiveness, chewiness and cohesiveness, were obtained. These parameters can reflect the quality characteristics of food products more comprehensively. The test method was modified concerning Battaiotto et al., (2020). P36R cylindrical probe was selected and the test program was cooked lasagne - PTA4 PFS.PRG. The test mode was the Adhesive test. Each set of tests was repeated three times.

The initial conditions for the surface viscosity determination of yam tablets were: pre-test speed of 1.00 mm/s, test speed of 2.00 mm/s, post-test speed of 2.00 mm/s, trigger force of 10.00 g, compressive degree of scaling of 75%, and data collection rate of 500 pps.

2.8. Moisture status

A low field-nuclear magnetic resonance (LF-NMR) analyzer was used to detect the moisture status in dried yam products under different drying methods. The dried yam products were placed in NMR tubes with an outer diameter of 1 in. and tested using a MesoMR core NMR analyzer. Transverse relaxation time (T_2) tests were performed using the Q - CPMG sequence.

The parameters for LF-NMR measurement of transverse relaxation time were modified from the test method of Guan et al., (2023). The parameters were as follows: the instrument temperature was maintained at 24 °C during the measurements, the magnetic field strength of the analyzer was 0.3 T, and the resonant frequency was SF = 12 MHz, the echo time TE = 0.2 ms, the relaxation decay time TW = 1500 ms, the number of accumulations NS = 8, the number of echoes NECH = 8000, and the 90°pulse times were: P90° = 7.00 μs, 180° pulse times: P180° = 11.04 μs.

2.9. Statistical analysis

The final results of each group of experimental data were taken from the mean of the data of three independent replicated experiments. One-way ANOVA was used to calculate the variability of the data on the drying rate of yam, total phenol content, allantoin content, and mechanical properties. $P < 0.05$ represents a statistically significant difference. Data results were expressed as mean ± standard deviation. The graphs were plotted using relevant software.

3. Results and analysis

3.1. Discharge characteristics in the EHD system

When high voltage is applied to the needle plate electrode of the EHD dryer, the tip of the needle discharges, ionizing the surrounding air into a plasma composed of free radicals and reactive atoms. The plasma emission spectra at different voltages are shown in Fig. 1a. The 200–900 cm^{-1} band in the spectrum mainly contains reactive nitrogen oxides (RONS). The intensity of the characteristic peaks in the emission spectra at different drying voltages represents the concentration of different RONS. This is because substances such as free radicals and reactive atoms are excited to an excited state under the action of high voltage. It is well known that substances in the excited state generally exist for only about 10^{-8} s and quickly jump to lower energy states (Deng et al., 2013). Each substance forms a different emission spectrum, so the intensity of the spectral lines is also affected by the voltage parameter. From Fig. 1a, it can be seen that the concentration of RONS increases with the increase in voltage. Among them, N_2* appeared at most of the strong peak positions such as near 307 nm, 328 nm, 349 nm, 372 nm, and 396 nm, N_2 appeared near 418 nm, 623 nm, 665 nm, and 751 nm, and weak peaks such as 288 nm, 585 nm, and 706 nm were at the positions of NO_γ^-, NO_2, and O_2, respectively (Chen et al., 2012). This phenomenon indicates that reactive nitrogen species is the main active substance in the emission spectrum of electrohydrodynamic discharge. Under the action of the non-uniform electric field, the motion of the above ions generates ionic wind. The size of the ionized wind is closely related to the drying rate. This is described in more detail below.

The discharge morphology and voltammetric characteristics of the EHD at different voltages are shown in Figs. 2c-e. The EHD voltage waveform is sinusoidal, and its peak value increases with the increase of voltage, while the current waveform shows that the discharge process belongs to the typical filamentary discharge pattern, and a large number of strong and dense current filaments can be seen, whose maximum amplitude increases with the voltage increase (Czech et al., 2011). This is because the current waveform is made up of many current pulses. Each current pulse represents a single discharge or a superposition of multiple discharges at that time. These pulses are characterized by high amplitude and short duration. Applying voltage to the upper pole plate begins to generate current, and the charged particles generated by the discharge in the first half of the cycle accumulate in large quantities on the surface of the lower plate, and when the voltage is reduced to the reverse, the electric field formed by these charges will contribute to the next half of the cycle. In a dark environment, a blue-violet glow can be observed during discharges of different voltages. The higher the voltage, the brighter the blue-violet glow. This indicates that the increase in voltage makes the discharge more pronounced.

From the voltage across the test capacitor and the electrode voltage, the Lissajous plot can be plotted for different voltages (Figs. 2f-h). Through the curve integration, we know that when the voltage is 13 kV, 17 kV and 21 kV, the area of the Lissajous plot is 0.141×10^6 V^2, 0.261×10^6 V^2 and 0.296×10^6 V^2, respectively. The size of the Lissajous pattern area increases with the increase of voltage. Therefore, from eq. (5), the discharge power of the EHD device also increases with the increase in voltage. This is because more energy is injected as the voltage increases, prompting the excitation-dissociation process of the gas to become more intense, benefiting the acquisition of more electrons and ions (Misra et al., 2014). When more charge can carry material, the current generated will increase, and the power will increase accordingly. According to the average drying time and average power, the average energy consumption of 13 kV, 17 kV, 21 kV and HAD can be calculated to be 253.80 kJ, 375.84 kJ, 319.68 kJ and 4800.0 kJ, respectively. The average energy consumption of EHD drying is significantly lower than that of HAD, which is a promising drying method. The average energy consumption of EHD drying is significantly lower than that of HAD, which is a promising drying method. In fact, the power (DC or AC) applied in EHD drying, the size of the voltage, the geometry and material of the electrode, and the distance between discharge and collection can all affect its energy efficiency. It was found that the drying efficiency of DC + was higher than that of AC, while the drying speed was much lower than that of AC (Singh al., 2016). The geometry of the discharge electrode also significantly affects the EHD drying efficiency. Under the condition of constant electric field intensity, the increase of

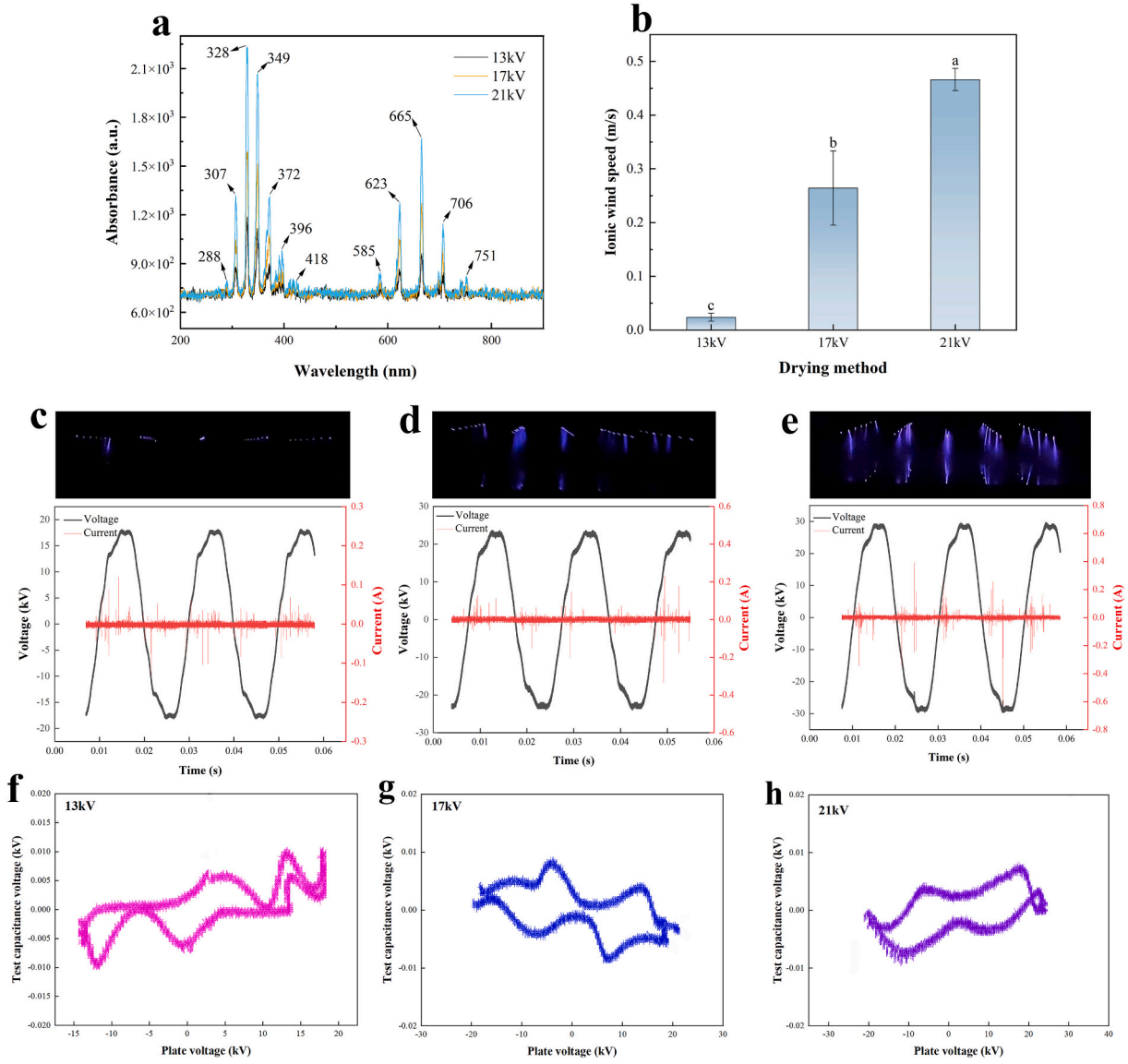

Fig. 1. Electric field discharge characteristics. a: Emission spectra at different drying voltages; b: Ion wind speed under different drying voltage; c-e: Discharge morphology and voltammetric characteristics at different drying voltages; f-h: Lissajous graphs at different drying voltages.

discharge spacing has a great influence on discharge power, which increases its energy efficiency (Bashkir al., 2020). Under the same high-pressure conditions, the energy efficiency of the multi-needle electrode is lower than that of the single-needle electrode, which is caused by the interference of the ion wind jet. However, the energy efficiency of multi-needle electrodes increases with the increase of needle spacing (Martynenko & Kudra, 2016a, 2016b; Martynenko & Zheng, 2016). Therefore, the needle spacing can be expanded to improve energy efficiency.

3.2. Drying characteristics

Fig. 2a and b show the curves of drying time and moisture content ratio of yam with time under different drying methods. We can see that different drying methods have significant effects on the moisture content ratio and drying time of yam ($P < 0.05$). The drying time of yam under different drying methods was different, but the moisture content ratio of yam showed an exponential decrease with the increase in drying time. At the early stage of drying, the moisture content ratio of yam decreased rapidly, and the decrease gradually slowed down with the extension of time. The fastest decrease in moisture content ratio was in the HAD. This was due to the high temperature destroying the internal tissue structure of the yam, resulting in the rupture of the internal capillary tissue structure of the yam and the violent contraction and cracking of the surface, thus reducing the resistance to diffusion of water from the inside of yam to the surface and speeding up the drying speed (Maskan et al., 2001). In the EHD treatment group, the ionic wind speed increased with the increase of the voltage (Fig. 1b), the decrease of moisture content of yam was accelerated and the drying time was reduced. EHD is a typical low-temperature drying. Drying is accomplished by the ionic wind generated under the action of an applied electric field impinging on the surface of the material. It is found that forced convection is beneficial to thermal drying due to the increase of boundary layer turbulence caused by forced convection, but it is not conducive to EHD drying because forced convection can significantly inhibit the positive effect of electric field on mass transfer (Martynenko & Kudra, 2016a, 2016b; Martynenko & Zheng, 2016). According to the study of Martynenko and Kudra (2016a), Martynenko and Kudra (2016b) and Martynenko and Zheng (2016), the Reynolds number is proportional to the ion wind speed. Under 21 kV drying, the ionized wind speed is the fastest, the Reynolds number is the largest, and the water content ratio of yam decreases the fastest. It indicates that the higher the Reynolds number the easier it is to

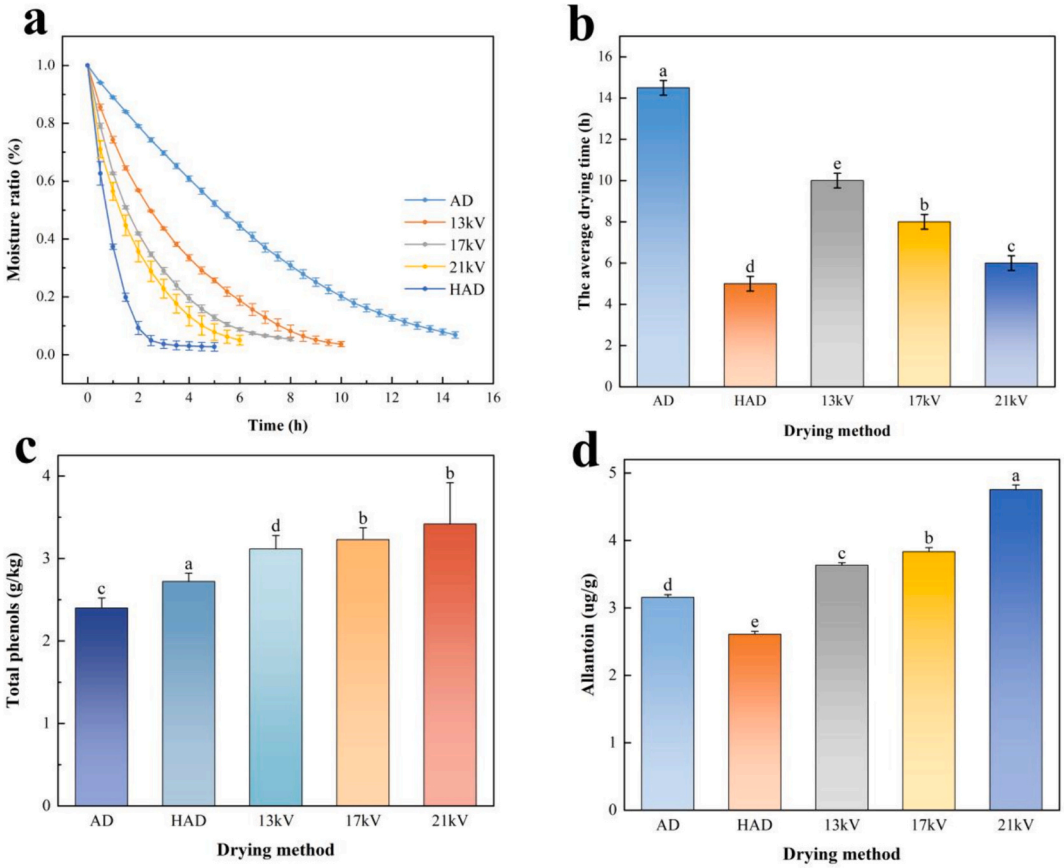

Fig. 2. Drying profiles, nutrient composition of yam under different drying methods. a: The curve of moisture content ratio of yam with time under different drying conditions; b: Average drying time of yam under different drying conditions; c: Total polyphenol content of yam under different drying conditions; d: Allantoin content of yam under different drying conditions; Note: Different letters indicate significant differences in the results ($P < 0.05$).

dry. Chokngamvong and Suvanjumrat (2023) had the same conclusion and they suggested that the reason why pineapple slices are difficult to dry at low Reynolds numbers is due to their need for higher activation energy. Another dimensionless Fourier number is determined by the drying time, which increases with decreasing moisture content. Rai and Upadhyay (2020) similarly found that evaporation of water from food products occurs faster when the Fourier number is higher. At the early stage of drying, the moisture on the surface of fresh yam evaporates rapidly under the action of ionic wind. The moisture inside the yam starts to transfer to the surface of the yam continuously. As drying proceeds, the moisture transported from the interior of the yam to the surface gradually decreases, and the moisture content ratio decreases as the moisture gradient decreases (Martynenko & Kudra, 2016a, 2016b; Martynenko & Zheng, 2016). Similarly, Xiao et al. (2015) had the same finding in the EHD drying of shiitake mushrooms, and they concluded that drying is a rate-reducing process.

3.3. Total polyphenol content (TPC)

The main reason for the antioxidant, antibacterial, antitumor, and immune-enhancing functions of yam is that it is rich in total phenols, and phenolic compounds are unstable and easily oxidized during drying (Khánh et al., 2020). The total polyphenol content in yam under different drying method treatments is shown in Fig. 2c. It has been found that TPC in plants is the main contributor to their antioxidant properties, and the correlation between antioxidant capacity and TPC is positive (Kalisz et al., 2020). The lowest TPC content was found in the AD treatment group, which was due to the longest drying time in the AD treatment group. Prolonged exposure to air not only decreases the antioxidant property of yam but also causes changes in the chemical structure of TPC, binding to proteins or other compounds. Also, temperature is one of the reasons affecting the TPC. It found that some phenolic compounds are more susceptible to heat than others, and they exist in hydrophilic regions of cells such as vesicles and extraplasmic bodies or act as soluble phenols in the cytoplasm and nucleus, and therefore most phenolic glycosides are protected by the cell wall (Yan & Kerr, 2012). However, the drying temperature of HAD is 60 °C. The thermal degradation effect under high temperatures destroys the integrity of the cell wall, leading to a decrease in TPC. The same finding was made by Maillard and Berset (1995), who attributed this phenomenon to the fact that high temperatures not only thermally release some of the phenolic acids that are bound to substances such as the cell wall that are insoluble in water, but also promote the degradation of lignin and other complex polysaccharides, which facilitates the phenolic acid release. There are also a few reports about date palms (Tepe & Ekinci, 2021) and blue honey suckleberry (Kalisz et al., 2020), which show that high temperatures will also destroy the antioxidant properties of plants, although the HAD time is short, it may also inactivate the enzymes of raw materials, namely polyphenol oxidase and peroxidase. These occurrences also promoted the thermal degradation of phenolics in yams dried in HAD. The TPC of dried yam products after EHD treatment was higher than that of HAD and AD, and the TPC increased with increasing voltage. This suggests that these yams are more beneficial to human health because they can help the human body avoid being attacked by dangerous free radicals. The TPC of the 21 kV was significantly higher than that of the other groups. The short drying time of EHD and the drying process will not raise the temperature can not only reduce the phenolic substances in the yam by the thermal effect of the impact can also better attenuate the oxidation, which is conducive to the retention of phenolic substances in the yam, to obtain a higher quality of yam.

3.4. Allantoin content

Allantoin is one of the major contributors to the medicinal value of yam. The allantoin capsule in yam is anesthetic and analgesic, anti-inflammatory and antibacterial, accelerates cell growth, promotes the healing of tissues in the body, and can soften keratin and repair tissues in the gastrointestinal tract when consumed regularly (Khánh et al., 2020). The allantoin content in yam after treatment with different drying methods is shown in Fig. 2d. The highest allantoin content was found in 21 kV, which had 1.24, 1.31, 1.51, and 1.82 times more allantoin than 17 kV, 13 kV, AD, and HAD, respectively. Allantoin is characterized by being extremely soluble in water (Zhang, Ding, et al., 2023; Zhang, Zheng, et al., 2023). From the previous analysis, we know that the drying time of the AD treatment group is the longest. This could be the reason for the loss of allantoin in AD. Allantoin originates from the degradation process of purines, and this process also involves xanthine oxidase, uricase and allantoinase (Chen, Lu, et al., 2017; Chen, Tian, et al., 2017). Therefore, the reason for the low allantoin content in the HAD may be the inhibition of enzyme activity under high-temperature conditions. Overall, EHD drying is more favorable for preserving allantoin in yam.

3.5. Textural property

Texture analysis has been widely used in food analysis in recent years. Texture change is an important cause of quality deterioration during the drying of solid foods, therefore texture profile analysis (TPA) has been used to measure and evaluate the textural properties of materials about people's senses, and its measurements are more accurate than sensory analysis (Battaiotto & Dello Staffolo, 2020). To investigate the effect of different methods of drying process on the texture of yam, we used TPA to puncture and analyze the dried yam products under different drying conditions, and obtained various physical indexes, such as hardness, elasticity, and chewiness of yam (Fig. 3). The effects of different drying methods on the textural properties of yam were significantly different ($P < 0.05$).

The magnitude of internal binding forces and the structure and content of proteins in yam are important factors affecting its textural properties (Al-Ali & Parthasarathy, 2020). From Figs. 3f-g, it can be seen that the textural properties of EHD were significantly better than those of HAD and AD. All the textural parameters of the yam after drying at 21 kV were optimal. Because EHD is a low-temperature drying, the process of water loss does not destroy the internal cellular structure of the yam, and the volatilization of water results in the reduction of the yam's volume, the molecular spacing becomes smaller, and the internal structure becomes more compact. The magnitude of cohesiveness is

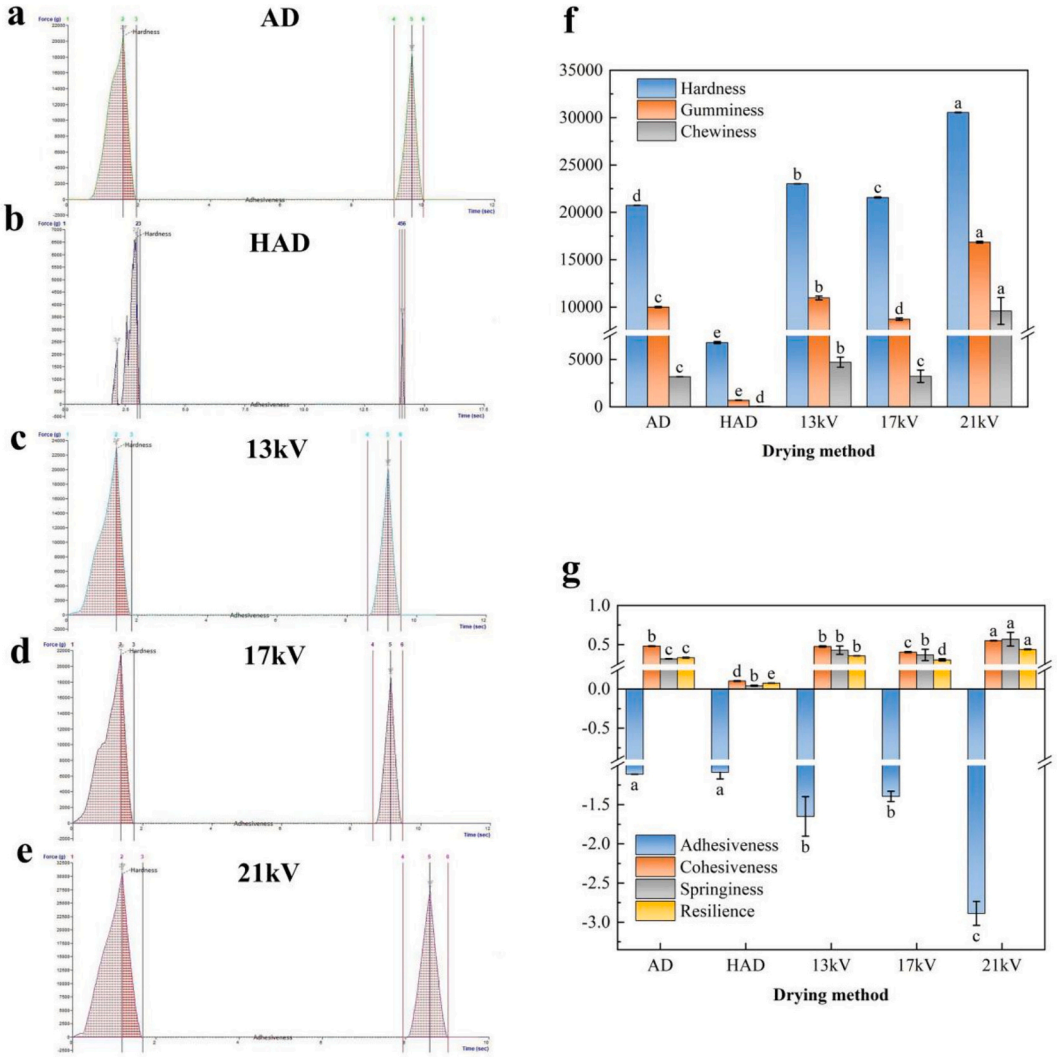

Fig. 3. Textural analysis of yam under different drying methods. a-e: Textural composition of yam under different drying conditions f: Hardness, gumminess, chewiness of yam under different drying conditions; g: Adhesiveness, cohesiveness, springness, resilience of yam under different drying conditions.

related to the protein structure inside the yam molecules (Katsoufi et al., 2020). As can be seen from Fig. 3g, the cohesiveness of the yam was the greatest after 21 kV drying, indicating that it had the greatest internal bonding and the finest texture. This is due to the maximum ionic wind speed and the concentration of each active particle during 21 kV drying (Figs. 1a and 2b), which includes ozone with strong oxidizing properties. Ozone has the effect of sterilization and disinfection. Similarly, it has been found that autoclave treatment increases the cohesiveness of sausages (Marcos et al., 2007). The protein content is an important factor affecting the springiness of yam (Trang et al., 2020). Fig. 3g shows that yam springness was best after 21 kV drying with the highest protein content. Adhesiveness and gumminess both reflect the intercellular bonding within the yam (Deguchi et al., 2021). Yam after 21 kV drying had high intercellular cohesion and the highest tissue tightness within the yam and therefore showed the maximum adhesiveness and gumminess. Chewiness is numerically expressed as the product of gumminess and springiness (Sun et al., 2019). Thus the yam after 21 kV drying sensationally showed a firm texture and was more sticky to the teeth. The HAD treatment group had the lowest yam adhesiveness and gumminess, which represented a smoother texture. The HAD treatment had the worst yam for all the textural parameters. The reason for this situation was that the high-temperature environment with rapid water loss damaged the internal organization of the yam, resulting in severe internal deformation, reduced intercellular cohesion, and dramatic surface shrinkage. It has been shown that both temperature and high-pressure environments affect the formation of protein aggregates. Compared with thermal drying, non-thermal drying can alleviate protein aggregation and degradation caused by high-temperature drying and improve the textural properties of dried products (Zhu et al., 2022). In addition, high-pressure treatment can increase the degree of protein aggregation, and the low-temperature and high-pressure EHD drying method was able to increase the degradation of myofibrillar proteins to antioxidant peptides in yam, which improved myofibrillar proteins' digestibility (Zhu et al., 2022). In our previous study, we found that the ordered structure α-helices and β-turns of proteins in yam were higher under EHD drying (Zhang, Ding, et al., 2023; Zhang, Zheng, et al., 2023). From Fig. 3b, it can be seen that there is a distinct peak in the curve of the HAD treatment group, which indicates the phenomenon of rupture of the yam tablets during the first compression, and this peak is expressed as the yam fracturability (Al-Ali & Parthasarathy, 2020). The fracturability of the yam after drying by HAD is 2275.793 N. The other method of drying post-yam did not show fracture at the first compression, so there was only one peak (Figs. 3a, c-e). Combining the hardness and fracturability of the yams after different drying methods, it can be concluded that the yams in the 21 kV treatment group are more suitable for transportation and are less prone to fracture during transportation.

3.6. Moisture status

The variation of low-field NMR spectra of dried yam products with drying time under different drying conditions is shown in Fig. 4. The shorter the relaxation time, the more tightly the moisture in the yam is bound to the yam, and the lower the degree of freedom of moisture in this state, the worse the mobility will be. On the contrary, the longer relaxation time represents the higher degree of freedom and the better fluidity. As can be seen from Fig. 4a, there are three more obvious absorption peaks in the T_2 relaxation profiles of dried yam products under different drying conditions. They represent different states of water fractions in yam, respectively. From left to right, they are T_{21} (0.01–1 ms), T_{22} (10–100 ms), and T_{23} (10–1500 ms). The T_{21} peak has the shortest relaxation time, which represents the bound water inside the dried yam product that is tightly bound to macromolecular substances such as cell wall starch, etc. (Chen et al., 2023). The relaxation time of the T_{22} peak represents the water that is not easily flowable inside the dried yam product that is trapped in a highly organized structure, with a degree of freedom between bound and free water, which is extremely easy to transform (Mowafy et al., 2024). The chemical exchange of water in the vesicles with sugars and other low-weight compounds that make up the dilute solution resulted in the longest relaxation time for peak T_{23}, representing free water present in the vesicles or extracellular space that is highly mobile (Zhu et al., 2018).

The peak areas covered by different T_2 signals in the T_2 spectra can be used to indicate the relative content of water in different states (Li et al., 2019). From Fig. 4b we can see that the content of bound water in dried yam products was significantly different after drying by different methods. The content of bound water in EHD drying increased with the increase of voltage. It is well known that the liquid bubble chamber should contain the maximum volume fraction of water. However, interestingly, observing the distribution of water states of bound water, less mobile water, and free water, it can be found that the free water gradually decreases with the increase of drying voltage. It indicates that under the action of high voltage, the water with a high degree of freedom is more easily removed and the bound water will be more compact. It has been shown that food moisture content can affect microbial growth and reproduction and the quality of food (Qin et al., 2017). In the process of food drying, water loss changes the original protein and cell structure, free water content decreases and bound water content increases, which inhibits the rate of microbial reproduction and growth. The lower the number and abundance of microbial colonies, the higher the quality of dried products. This phenomenon has also been verified in the drying of apples, lotus seeds, etc. (Hills & Remigereau, 2003; Mothibe et al., 2014). The yam in HAD is exposed to high temperatures for a long period, and the temperature is too high for the loss of water to occur too quickly. The process of diffusion of water from the interior of yam to the surface leads to damage and rupture of its internal

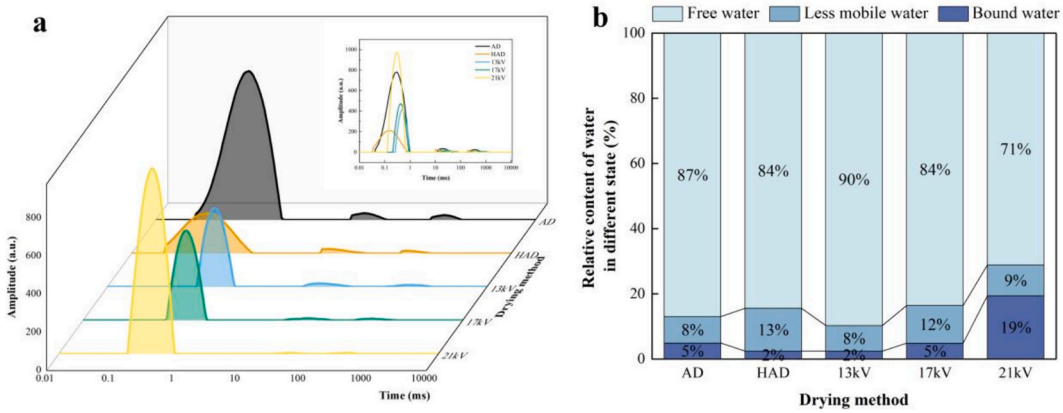

Fig. 4. Low-field NMR of yam. a: Transverse relaxation time T_2 profiles of yam under different drying conditions; b: Proportion of water in different states in yam.

capillary tissue structure, violent contraction and cracking of the surface, and the loss of water in the vesicles accompanied by a reduction in the overall volume of the whole cell, which affects the distribution and migration of its water (Maskan, 2001). Some studies also obtained the same conclusion. When analyzing the distribution and migration of water in cherries during storage, it is found that the temperature difference during storage will lead to the change of chemical composition in cherry, which will lead to the migration of water in cytoplasm and vacuole with the extension of storage time (Zhu et al., 2018). It has also been found that high drying temperatures or fast drying rates can lead to deterioration in the quality of rice seeds, resulting in internal cracks at the seedling stage (Wang et al., 2021). In addition, when the needle tip discharge is enhanced in EHD drying, breaking causes energy-carrying ions generated by ionization of the surrounding air to enter into the yam, interacting with the macromolecules and water molecules in the yam, and enhancing the binding capacity of the macromolecules and water molecules. It is also important to note that EHD is a low-temperature drying, and the ionized air only acts on the surface of the yam and does not damage the internal structure of the yam. Therefore, the drying mainly targets the moisture with a high degree of freedom.

3.7. Statistical analysis

In order to better illustrate the effects of different drying methods on all indicators of yam, the correlation coefficients between different drying methods and all indicators of yam were obtained after normalizing all experimental data by z-score (Fig. 5a). Through Fig. 5a we can get the correlation coefficients between different drying methods and all indicators of yam. From Fig. 5a, we can see that the total phenol and allantoin contents were positively correlated with the EHD treatment group and negatively correlated with the AD and HAD treatment groups. It indicates that EHD is more favorable to preserve the nutrients inside the yam. The positive correlation coefficients of hardness, adhesiveness, gumminess, chewiness, cohesiveness, springiness, and resilience were the largest in the 21 kV treatment group compared with other methods. It indicates that yam dried at 21 kV has the tightest internal cell structure and the best textural properties. The above values were negatively correlated with HAD, and the excessive temperature led to damage to the internal cell structure of the yam, which had a great impact on the textural properties of the yam. Fig. 5b shows Pearson's correlation coefficient matrix between different indicators of yam under different drying methods, which is used to represent the correlation coefficients between different indicators of yam. Hardness was positively correlated with gumminess, chewiness, cohesiveness, springiness, and resilience. It indicates that the higher the value of hardness, the better the intercellular bonding, and the better gumminess, chewiness, cohesiveness, springiness, and resilience the yam will possess. Fig. 5c and d show the radar charts of each group. From the area surrounded by the radar plot, it can be known that EHD drying at 21 kV is the most suitable drying method for yam.

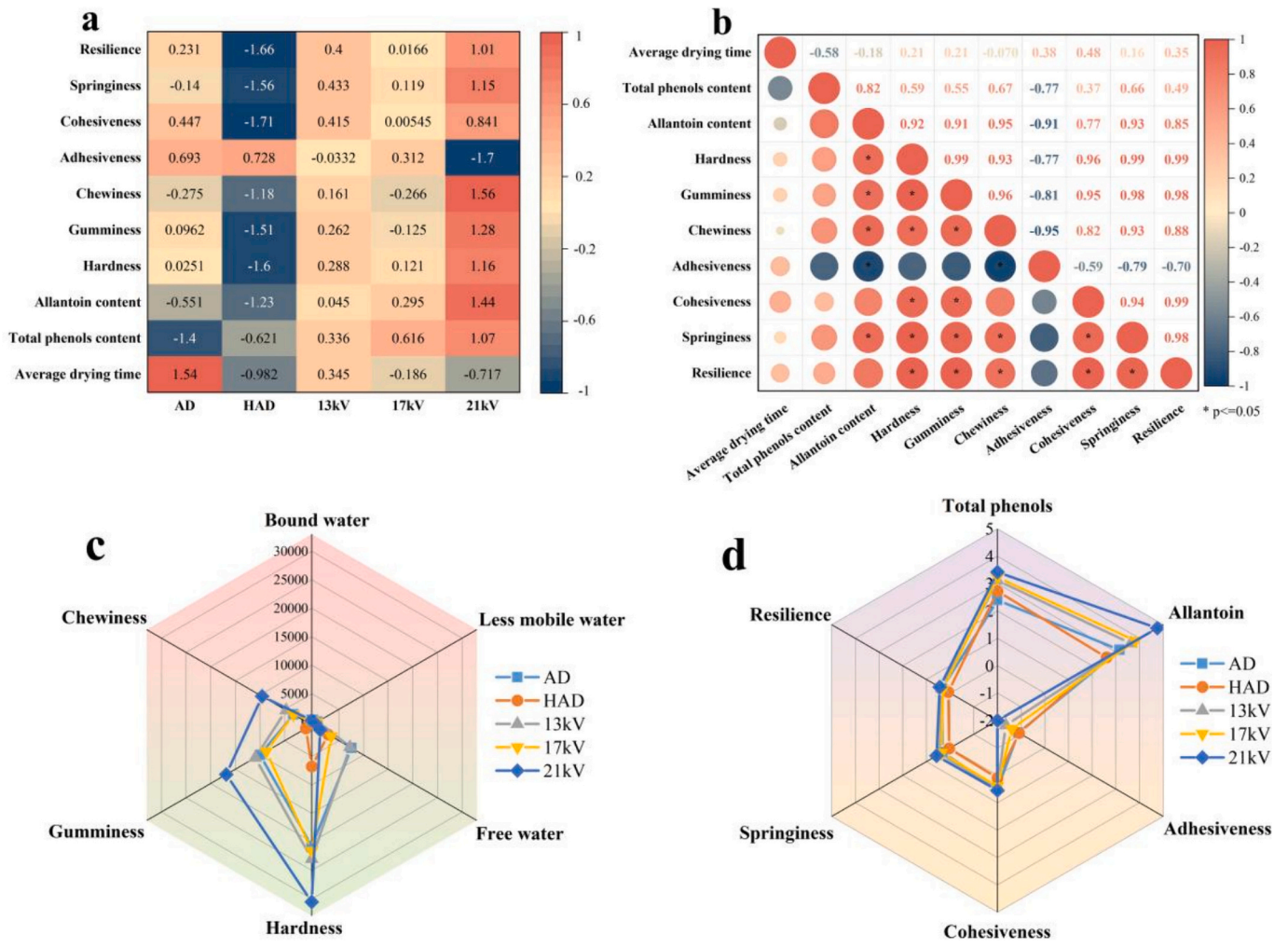

Fig. 5. Statistical analyses. a: Thermogram of correlation between different drying methods and drying index of yam; b: Pearson's correlation coefficient matrix. c-d: Radar plots.

4. Conclusions

In this study, we investigated the effects of different drying methods (EHD, AD, HAD) on the drying quality, quality parameters (e.g., total phenol content, allantoin content), texture characteristics and moisture distribution of yam. The results showed that the electrohydrodynamic discharge device could produce a rich variety of plasma actives. The concentration of RONS produced during the discharge process, the ion wind speed, the intensity of the emission spectrum, and the discharge power all increased with the increase of voltage. The moisture ratio of yam in the HAD decreased at the fastest rate. And the drying time was 5 h, which was 20%–65.51% shorter than EHD and AD. Different drying methods resulted in different binding states and distribution of water within the yam. Free water was more easily removed and bound water would be more tightly bound in high-voltage drying. The textural properties of yam were affected by drying temperature and drying time. Due to the faster drying speed and low drying temperature of EHD, the integrity of the internal structure of the yam will not be damaged. Therefore, the hardness, gumminess, chewiness, adhesiveness, cohesiveness, springiness, and resilience of the yam are the best after 21 kV drying. The advantages of low-temperature drying make EHD drying play a positive advantage in retaining the nutrients of yam. It could increase the total polyphenol content of dried yam products by 1.25–1.42 times and allantoin content by 1.51–1.82 times. In conclusion, these findings are conducive to making EHD drying, a non-thermal processing technology, more widely used in the industry, providing a theoretical basis and experimental validation for industrialization to improve the quality of dried yam products, and laying a foundation for further upgrading and industrialization of EHD drying technology.

CRediT authorship contribution statement

Changjiang Ding: Writing – review & editing, Supervision, Resources, Project administration, Conceptualization. **Jingli Lu:** Writing – review & editing, Supervision, Resources, Project administration, Conceptualization. **Jie Zhu:** Writing – original draft, Methodology, Investigation, Conceptualization. **Wurile Bai:** Visualization, Validation, Data curation. **Peng Guan:** Visualization, Validation, Data curation. **Zhiqing Song:** Methodology, Conceptualization. **Hao Chen:** Methodology, Conceptualization.

Declaration of competing interest

The authors declare that they have no known competing financial interests or personal relationships that could have appeared to influence the work reported in this paper.

Data availability

Data will be made available on request.

Acknowledgements

The authors are grateful for the support provided by National Natural Science Foundations of China (Nos. 12365023, 52067017 and 12265021), Program for Young Talents of Science and Technology in Universities of Inner Mongolia Autonomous Region (No. NJYT23020), Natural Science Foundation of Inner Mongolia Autonomous Region (Nos. 2022LHMS01002 and 2023LHMS05019), The Basic Scientific Research Business Project of the Universities Directly of the Inner Mongolia Autonomous Region of China (Nos. ZTY2024082, JY20220066, JY20220232, JY20240045 and JY20240070). The authors also would like to express their gratitude to the anonymous referees for their valuable comments and suggestions.

References

Al-Ali, M., & Parthasarathy, R. (2020). Influence of microwave drying and conventional drying methods on the mechanical properties of naproxen sodium drug tablets. *Particuology, 53*, 30–40. https://doi.org/10.1016/j.partic.2020.01.006

Battaiotto, L. L., & Dello Staffolo, M. (2020). Drying kinetics, microstructure, and texture of cheese cracker fillings. *Food and Bioproducts Processing, 123*, 199–208. https://doi.org/10.1016/j.fbp.2020.06.014

Chauhan, A., Singh, S., Dhar, A., & Powar, S. (2021). Optimization of pineapple drying based on energy consumption, nutrient retention, and drying time through multi-criteria decision-making. *Journal of Cleaner Production, 292*, Article 125913. https://doi.org/10.1016/j.jclepro.2021.125913

Chen, L., Tian, Y., Sun, B., Wang, J., Tong, Q., & Jin, Z. (2017). Rapid, accurate, and simultaneous measurement of water and oil contents in the fried starchy system using low-field NMR. *Food Chemistry, 233*, 525–529. https://doi.org/10.1016/j.foodchem.2017.04.147

Chen, L., Wei, Y., Zuo, X., Cong, J., & Meng, Y. (2012). The atmospheric pressure air plasma jet with a simple dielectric barrier. *Thin Solid Films, 521*, 226–228. https://doi.org/10.1016/j.tsf.2011.11.069

Chen, P., Li, Y., Jiang, M., Zhu, W., Wang, D., Chen, L., & Zhang, R. (2023). Use of low-field nuclear magnetic resonance for moisture variation analysis of fresh in-shell peanut during different drying methods. *Journal of Food Process Engineering, 46*(12), Article e14486. https://doi.org/10.1111/jfpe.14486

Chen, X., Lu, J., Li, X., Wang, Y., Miao, J., Mao, X., … Gao, W. (2017). Effect of blanching and drying temperatures on starch-related physicochemical properties, bioactive components and antioxidant activities of yam flours. *LWT - Food Science and Technology, 82*, 303–310. https://doi.org/10.1016/j.lwt.2017.04.058

Chokngamvong, S., & Suvanjumrat, C. (2023). Study of drying kinetics and activation energy for drying a pineapple piece in the crossflow dehydrator. *Case Studies in Thermal Engineering, 49*, Article 103351. https://doi.org/10.1016/j.csite.2023.103351

Czech, T., Sobczyk, A. T., & Jaworek, A. (2011). Optical emission spectroscopy of point-plane corona and back-corona discharges in air. *The European Physical Journal D, 65* (3), 459–474. https://doi.org/10.1140/epjd/e2011-20196-x

Deguchi, M., Ito, S., Motohashi, R., & Arai, E. (2021). Effects of taro (*Colocasia esculenta* L. Schott) drying on the properties of taro flour and taro flour products. *Food Science and Technology Research, 27*(3), 369–379. https://doi.org/10.3136/fstr.27.369

Deng, X. L., Nikiforov, A. Y., Vanraes, P., & Leys, C. (2013). Direct current plasma jet at atmospheric pressure operating in nitrogen and air. *Journal of Applied Physics, 113* (2), Article 023305. https://doi.org/10.1063/1.4774328

Ferreira, D., Silva, J. A. L.d., Pinto, G., Santos, C., Delgadillo, I., & Coimbra, M. A. (2007). Effect of sun-drying on microstructure and texture of S. Bartolomeu pears (*Pyrus communis* L.). *European Food Research and Technology, 226*(6), 1545–1552. https://doi.org/10.1007/s00217-007-0685-x

Guan, Y., Hua, Z., Cheng, Y., He, J., Zhang, Y., & Guan, J. (2023). Monitoring of water content of apple slices using low-field nuclear magnetic resonance during drying process. *Journal of Food Process Engineering, 46*(12), 14445. https://doi.org/10.1111/jfpe.14445

Hills, B. P., & Remigereau, B. (2003). NMR studies of changes in subcellular water compartmentation in parenchyma apple tissue during drying and freezing. *International Journal of Food Science & Technology, 32*(1), 51–61. https://doi.org/10.1046/j.1365-2621.1997.00381.x

Ju, H.-Y., El-Mashad, H. M., Fang, X.-M., Pan, Z., Xiao, H.-W., Liu, Y.-H., & Gao, Z.-J. (2015). Drying characteristics and modeling of yam slices under different relative humidity conditions. *Drying Technology, 34*(3), 296–306. https://doi.org/10.1080/07373937.2015.1052082

Ju, H.-Y., Zhang, Q., Mujumdar, A. S., Fang, X.-M., Xiao, H.-W., & Gao, Z.-J. (2016). Hot-air drying kinetics of yam slices under step change in relative humidity. *International Journal of Food Engineering, 12*(8), 783–792. https://doi.org/10.1515/ijfe-2015-0340

Kalisz, S., Oszmiański, J., Kolniak-Ostek, J., Grobelna, A., Kieliszek, M., & Cendrowski, A. (2020). Effect of a variety of polyphenols compounds and antioxidant properties of rhubarb (*Rheum rhabarbarum*). *Lwt, 118*, Article 108775. https://doi.org/10.1016/j.lwt.2019.108775

Katsoufi, S., Lazou, A. E., Giannakourou, M. C., & Krokida, M. K. (2020). Air drying kinetics and quality characteristics of osmodehydrated-candied pumpkins using alternative sweeteners. *Drying Technology, 39*(16), 2194–2205. https://doi.org/10.1080/07373937.2020.1760296

Khánh, H. H. N., Manh, T. D., Minh, T. N., Thinh, P. V., Cong, N. T., & Tuyen, K. C. (2020). Effects of various drying methods on physicochemical characteristics, flavonoids and polyphenol content, and antioxidant activities of different extracts from Morinda citrifolia fruit. *Journal of Pharmaceutical Research International, 32*(37), 72–82. https://doi.org/10.9734/jpri/2020/v32i3731005

Krokida, M. K., Karathanos, V. T., & Maroulis, Z. B. (2000). Compression analysis of dehydrated agricultural products. *Drying Technology, 18*(1–2), 395–408. https://doi.org/10.1080/07373930008917711

Li, L., Zhang, M., & Yang, P. (2019). Suitability of LF-NMR to analysis water state and predict dielectric properties of Chinese yam during microwave vacuum drying. *LWT - Food Science and Technology, 105*, 257–264. https://doi.org/10.1016/j.lwt.2019.02.017

Maillard, M. N., & Berset, C. (1995). Evolution of antioxidant activity during kilning: Role of insoluble bound phenolic acids of barley and malt. *Journal of Agricultural and Food Chemistry, 43*(7), 1789–1793. https://doi.org/10.1021/jf00055a008

Marcos, B., Aymerich, T., Dolors Guardia, M., & Garriga, M. (2007). Assessment of high hydrostatic pressure and starter culture on the quality properties of low-acid

fermented sausages. *Meat Science, 76*(1), 46–53. https://doi.org/10.1016/j.meatsci.2006.09.020

Martynenko, A., & Janaszek, M. A. (2014). Texture changes during drying of apple slices. *Drying Technology, 32*(5), 567–577. https://doi.org/10.1080/07373937.2013.845573

Martynenko, A., & Kudra, T. (2016a). Electrohydrodynamic (EHD) drying of grape pomace. *Japan Journal of Food Engineering, 17*(4), 123–129. https://doi.org/10.11301/jsfe.17.123

Martynenko, A., & Kudra, T. (2016b). Electrically-induced transport phenomena in EHD drying - A review. *Trends in Food Science & Technology, 54*, 63–73. https://doi.org/10.1016/j.tifs.2016.05.019

Martynenko, A., & Zheng, W. (2016). Electrohydrodynamic drying of apple slices: Energy and quality aspects. *Journal of Food Engineering, 168*, 215–222. https://doi.org/10.1016/j.jfoodeng.2015.07.043

Maskan, M. (2001). Drying, shrinkage and rehydration characteristics of kiwifruits during hot air and microwave drying. *Journal of Food Engineering, 48*, 177–182. https://doi.org/10.1016/S0260-8774(00)00155-2

Misra, N. N., Patil, S., Moiseev, T., Bourke, P., Mosnier, J. P., Keener, K. M., & Cullen, P. J. (2014). In-package atmospheric pressure cold plasma treatment of strawberries. *Journal of Food Engineering, 125*, 131–138. https://doi.org/10.1016/j.jfoodeng.2013.10.023

Mothibe, K. J., Zhang, M., Mujumdar, A. S., Wang, Y. C., & Cheng, X. (2014). Effects of ultrasound and microwave pretreatments of apple before spouted bed drying on rate of dehydration and physical properties. *Drying Technology, 32*(15), 1848–1856. https://doi.org/10.1080/07373937.2014.952381

Mowafy, S., Guo, J., Lei, D., & Liu, Y. (2024). Application of novel blanching and drying technologies improves the potato drying kinetics and maintains its physicochemical attributes and flour functional properties. *Innovative Food Science & Emerging Technologies, 94*, Article 103648. https://doi.org/10.1016/j.ifset.2024.103648

Ni, J., Ding, C., Zhang, Y., & Song, Z. (2020). Impact of different pretreatment methods on drying characteristics and microstructure of goji berry under electrohydrodynamic (EHD) drying process. *Innovative Food Science & Emerging Technologies, 61*, Article 102318. https://doi.org/10.1016/j.ifset.2020.102318

Ni, J.-B., Bi, Y.-X., Vidyarthi, S. K., Xiao, H.-W., Han, L.-D., Wang, J., & Fang, X.-M. (2023). Non-thermal electrohydrodynamic (EHD) drying improved the volatile organic compounds of lotus bee pollen via HS-GC-IMS and HS-SPME-GC-MS. *Lwt, 176*, Article 114480. https://doi.org/10.1016/j.lwt.2023.114480

Ni, J.-B., Wang, Y.-C., Xiao, H.-W., Zielinska, S., Tian, W.-L., Li, X.-X., … Fang, X.-M. (2023). Effect of electrohydrodynamic drying on bee pollen biochemical pathways. *Journal of Cleaner Production, 428*, Article 139358. https://doi.org/10.1016/j.jclepro.2023.139358

Paul, A., & Martynenko, A. (2022). The effect of material thickness, load density, external airflow, and relative humidity on the drying efficiency and quality of EHD-dried apples. *Foods, 11*(18), 2765. https://doi.org/10.3390/foods11182765

Polat, A., & Izli, N. (2020). Determination of drying kinetics and quality parameters for drying apricot cubes with electrohydrodynamic, hot air and combined electrohydrodynamic-hot air drying methods. *Drying Technology, 40*(3), 527–542. https://doi.org/10.1080/07373937.2020.1812633

Qin, N., Zhang, L., Zhang, J., Song, S., Wang, Z., Regenstein, J. M., & Luo, Y. (2017). Influence of lightly salting and sugaring on the quality and water distribution of grass carp (*Ctenopharyngodon idellus*) during super-chilled storage. *Journal of Food Engineering, 215*, 104–112. https://doi.org/10.1016/j.jfoodeng.2017.07.011

Rai, K. N., & Upadhyay, S. (2020). A mathematical model on heat mass transfer including relaxation time for different geometries during drying of foods. *Journal of Heat Transfer, 142*(9), Article 092102. https://doi.org/10.1115/1.4047147

Song, S., Zhang, Z., Zou, N., Chen, R., Han, L., Pan, C., & Sapozhnikova, Y. (2017). Determination of six paraben residues in fresh-cut vegetables using QuEChERS with multi-walled carbon nanotubes and high-performance liquid chromatography–tandem mass spectrometry. *Food Analytical Methods, 10*(12), 3972–3979. https://doi.org/10.1007/s12161-017-0970-7

Sun, K.-N., Liao, A.-M., Zhang, F., Thakur, K., Zhang, J.-G., Huang, J.-H., & Wei, Z.-J. (2019). Microstructural, textural, sensory properties and quality of wheat-yam composite flour noodles. *Foods, 8*(10), 519. https://doi.org/10.3390/foods8100519

Tepe, B., & Ekinci, R. (2021). Drying characteristics and some quality parameters of whole jujube (*Zizyphus jujuba mill.*) during hot air drying. *Italian. Journal of Food Science, 33*(1), 1–15. https://doi.org/10.15586/ijfs.v33i1.1947

Trang, B. M., Lan, S. Y., Park, J. H., Jang, H. W., Kim, K. M., Cho, Y. S., … Kim, H. Y. (2020). The effects of pretreatment methods on quality characteristic of hot air-dried sweet potato slices. *Food Engineering Progress, 24*(3), 164–170. https://doi.org/10.13050/foodengprog.2020.24.3.164

Wang, C., Zhang, Y., Liu, S., Yin, Y., Fan, G.-C., Shen, Y., … Wang, W. (2023). Allosteric probe-triggered isothermal amplification to activate CRISPR/Cas12a for sensitive electrochemiluminescence detection of Salmonella. *Food Chemistry, 425*, Article 136382. https://doi.org/10.1016/j.foodchem.2023.136382

Wang, H., Che, G., Wan, L., Liu, M., & Sun, W. (2021). Experimental study on drying characteristics of rice by low-field nuclear magnetic resonance. *Journal of Food Process Engineering, 44*(6), 13705. https://doi.org/10.1111/jfpe.13705

Xiao, H.-W., Bai, J.-W., Xie, L., Sun, D.-W., & Gao, Z.-J. (2015). Thin-layer air impingement drying enhances drying rate of American ginseng (*Panax quinquefolium* L.) slices with quality attributes considered. *Food and Bioproducts Processing, 94*, 581–591. https://doi.org/10.1016/j.fbp.2014.08.008

Yan, H., & Kerr, W. L. (2012). Total phenolics content, anthocyanins, and dietary fiber content of apple pomace powders produced by vacuum-belt drying. *Journal of the Science of Food and Agriculture, 93*(6), 1499–1504. https://doi.org/10.1002/jsfa.5925

Zhang, J., Ding, C., Lu, J., Wang, H., Bao, Y., Han, B., … Chen, H. (2023). Influence of electrohydrodynamics on the drying characteristics and volatile components of iron stick yam. *Food Chemistry: X, 20*, Article 101026. https://doi.org/10.1016/j.fochx.2023.101026

Zhang, J., Zheng, X., Xiao, H., Li, Y., & Yang, T. (2023). Effect of combined infrared hot air drying on yam slices: Drying kinetics, energy consumption, microstructure, and nutrient composition. *Foods, 12*(16), 3048. https://doi.org/10.3390/foods12163048

Zhu, D., Liang, J., Liu, H., Cao, X., Ge, Y., & Li, J. (2018). Sweet cherry softening accompanied with moisture migration and loss during low-temperature storage. *Journal of the Science of Food and Agriculture, 98*(10), 3651–3658. https://doi.org/10.1002/jsfa.8843

Zhu, Z., Pius Bassey, A., Cao, Y., Ma, Y., Huang, M., & Yang, H. (2022). Food protein aggregation and its application. *Food Research International, 160*, Article 111725. https://doi.org/10.1016/j.foodres.2022.111725